Orientation-Dependent Electron Transfer Processes in Fullerene−Aniline Dyads

K. George Thomas,*[†,‡] V. Biju,[†] D. M. Guldi,[‡] Prashant V. Kamat,*[,‡] and M. V. George[†,‡,§]

Photochemistry Research Unit, Regional Research Laboratory (CSIR), Trivandrum 695 019, India, Radiation Laboratory, University of Notre Dame, Notre Dame, Indiana 46556, and Jawaharlal Nehru Centre for Advanced Scientific Research, Bangalore 560 012, India

Received: July 14, 1999; In Final Form: October 5, 1999

Newly synthesized ortho- and para-substituted fullerene−aniline dyads exhibit orientation-dependent electron transfer under photoexcitation. Minimum energy conformation based on molecular mechanics calculations yield folded conformations for ortho-substituted dyads and extended ones for the para-substituted dyads. ^{1}H NMR studies also provided evidence for the folding of the anilinic group in the case of ortho-substituted dyads. Through-space charge transfer processes in these dyads were investigated using steady state fluorescence and lifetime measurements. The decrease in the spatial distance between the donor and acceptor moieties of the ortho-substituted dyads facilitated an efficient electron transfer. The marked increase in the singlet excited state deactivation rate constants and quantum yields of charge separation observed in the case of the ortho-substituted dyads, in polar solvents, further support a topographically controlled electron transfer process.

Introduction

Light-induced electron transfer processes play a key role in photosynthetic systems[1] and in the design of artificial molecular devices based on donor−acceptor pairs.[2] Energetics, distance and orientation between the donor and acceptor moieties, nature of the spacer, solvent, and temperature are some of the important parameters that control light-induced charge separation in these dyads. One of the ultimate aims of studies on donor−acceptor systems is to develop devices that can convert light energy into electricity or fuels.

Recent studies have shown that C_{60} is a suitable candidate to be employed as an electron acceptor in the design of donor−bridge−acceptor [D−B−A] systems.[3] The photoinduced charge transfer processes in fullerene-based dyads and triads have received considerable attention.[4−8] In all of these systems, the singlet or triplet excited state of the photoexcited C_{60} accepts an electron from the linked donor group to give the charge-separated state. In the case of fullerene-donor dyads, extending the lifetime of the charge-separated state, by controlling the rates of forward and back electron transfer, has been a challenging task.

Several strategies[9] have been adopted for the design of D−B−A systems, which can generate long-lived, charge separated states with high efficiency and slow charge recombination rates. In the case of natural photosynthetic systems, one of the prime factors responsible for the high efficiency of electron transfer is the well-defined orientation of chromophoric units in the protein matrices.[1] Effects of orientation of donor and acceptor moieties on electron transfer processes in porphyrin−quinone model systems have been reported.[9a−c] It was proposed in these studies that the nature of the bridging groups used in the D−B-A systems plays a significant role in controlling the orientation and distance of separation of the donor−acceptor pair. In a recent work, Imahori and co-workers have studied the effect of the linkage and solvent dependence on the photoinduced electron transfer processes in a series of zincporphyrin−C_{60} dyads.[5e]

Solvent-dependent intermolecular photoinduced electron transfer between substituted pyrrolidinofullerenes and *N*,*N*′-dimethylaniline has been recently reported by Luo et al.[10] In a recent study, we characterized the excited-state properties of a para-substituted fullerene−aniline dyad.[8a] We failed to observe any charge transfer products upon photoexcitation of this para-substituted dyad in neat solvents. However, upon clustering these dyads, in mixed solvents, yielded remarkably stable charge transfer products which lived for several hundreds of microseconds.[8b] The remarkable stability of the charge-separated intermediates in the clustered dyads is attributed to the hopping of the electron between the fullerene molecules. Similarly, rigid donor−bridge−C_{60} systems with extended hydrocarbon bridges were reported to exhibit charge separated states under photoexcitation.[4] These observations prompted us to probe how the orientation of donor−acceptor moieties influence the intramolecular electron transfer in fullerene−aniline based dyads. Examples of orientation effects that control the photoinduced electron transfer in a series of fullerene based D−B−A systems are reported here. The difference in orientation between donor−acceptor moieties has been achieved by attaching an anilinic donor to the ortho as well as para positions of the phenyl groups of 1-methyl-2-phenylpyrrolidinofullerene, using ethylenic and propylenic linkers (**1**−**4** in Chart 1). With the use of steady state and time-resolved fluorescence techniques, the forward electron transfer properties in these dyads were examined in polar and nonpolar solvents.

Experimental Section

All melting points are uncorrected and were determined on a Aldrich melting point apparatus. IR spectra were recorded on a Perkin-Elmer model 882 IR spectrometer and UV−visible spectra on a Shimadzu 2100 or GBC 918 spectrophotometer. ^{1}H NMR and ^{13}C NMR spectra were recorded either on a JEOL EX-90 MHz spectrometer or a Bruker DPX-300 MHz spec-

[†] Regional Research Laboratory.
[‡] University of Notre Dame.
[§] Jawaharlal Nehru Centre for Advanced Scientific Research.

10.1021/jp992369k CCC: $18.00 © 1999 American Chemical Society
Published on Web 11/10/1999

CHART 1

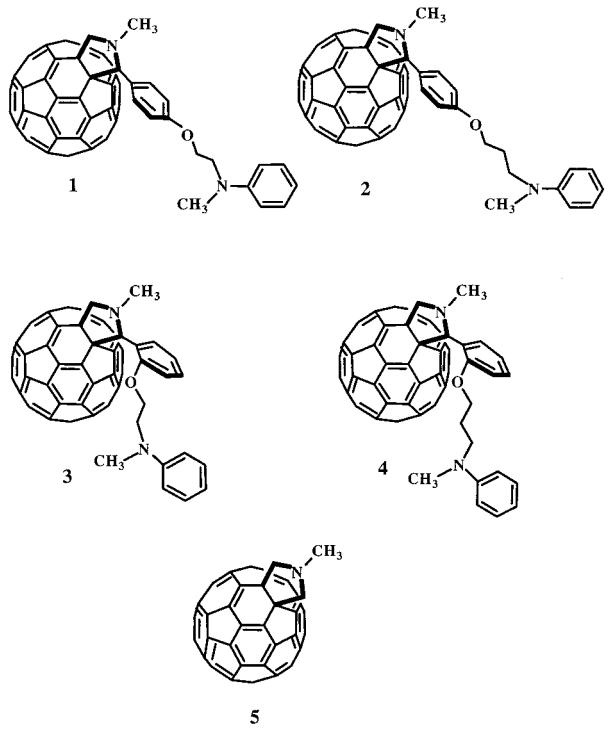

trometer. The emission spectra were recorded on a Spex-Fluorolog, F112-X equipped with a 450 W, Xe lamp and a Hamamatsu R928 photomultiplier tube. The excitation and emission slits were 1 and 4 nm, respectively. A 570-nm long pass filter was placed before the emission monochromator in order to eliminate the interference from the solvent. Solvent spectra were recorded in each case and subtracted. Quantum yields of fluorescence were measured by a relative method using optically dilute solutions (absorbance adjusted to 0.1 at 470 nm). *N*-Methylpyrrolidinofullerene dissolved in toluene ($\phi_f = 6.0 \times 10^{-4}$) was used as reference.[4,7a] All of the lifetimes and rate constants reported in this study are within the experimental error of ± 5%.

Synthesis of Fullerene−Aniline Dyads 2−4. The general method adopted for the synthesis of fullerene−aniline dyads is shown in Scheme 1. The purity of all these dyads was confirmed by HPLC.[11] Reported procedures were followed for the preparation of *N*-methyl,*N*-{(2-bromo)-1-ethyl}aniline (**7**),[8a] *N*-methyl, *N*-{(*p*-formylphenoxy)-1-ethyl}aniline (**9**),[8a] fullerene−aniline dyad (**1**)[8a] and model compound, *N*-methylpyrrolidinofullerene (**5**).[12a]

***N*-Methyl,*N*-{(3-bromo)-1-propyl}aniline (10).**[12b] To an ice-cold solution of *N*-methyl,*N*-{(3-hydroxy)-1-propyl}aniline (15 mmol) in dichloromethane (20 mL) was added PBr_3 (15 mmol), dropwise over a period of 1 h. The reaction mixture was further stirred at room temperature for an additional period of 3 h. The reaction was quenched with ice-cold water and the pH was adjusted to 7−8. The organic portion was extracted with dichloromethane and the solvent was removed under vacuum. The crude product was chromatographed on silica gel (100−200 mesh) using a mixture (1:20) of ethyl acetate and petroleum ether (bp 60−80 °C) to give 3.06 g (90%) of **10**; IR (neat) ν_{max} 3037, 2954, 2827, 1605, 1508, 1445, 1369, 1257, 1222, 1109, 1030, 992, 751 cm^{-1}; ^1H NMR ($CDCl_3$) δ 1.8−2.3 (2H, m, CH_2), 2.95 (3H, s, NCH_3), 3.2−3.6 (4H, m, NCH_2 and $BrCH_2$), 6.5−7.4 (5 H, m, aromatic); ^{13}C NMR ($CDCl_3$) δ 29.98, 31.29, 38.60, 50.89, 112.35, 116.50, 129.15, 149.02; exact mass calcd. for $C_{10}H_{14}NBr$ ($M^{\bullet+}$) 227.0310, found 227.0313 (FAB high-resolution mass spectrometry).

General Method of Preparation of *N*-Methyl,*N*-{(formylphenoxy)alkyl}anilines (8, 11, 12, 13). A mixture of the appropriate bromide (5 mmol), hydroxybenzaldehyde (5 mmol) and potassium carbonate (5 mmol) was refluxed in dry acetone (15 mL) for 12 h. The reaction mixture was cooled, filtered, and concentrated under reduced pressure. The crude product was chromatographed over silica gel (100−200 mesh) in each case.

*Compound **8***. Elution of the column with a mixture (1:10) of ethyl acetate and hexane gave 750 mg (60%) of **8**. IR (neat) ν_{max} 2934, 2762, 2794, 1692, 1604, 1500, 1460, 1368, 1292, 1243, 1039, 832 cm^{-1}; ^1H NMR ($CDCl_3$) δ 3.05 (3H, s, NCH_3), 3.7−3.9 (2H, t, NCH_2), 4.1−4.3 (2H, t, OCH_2), 6.6−7.9 (9H, m, aromatic), 10.4 (1H, s, CHO); ^{13}C NMR ($CDCl_3$) δ 39.02, 51.55, 65.90, 112.06, 112.18, 116.68, 120.77, 124.74, 128.26, 129.18, 135.75, 148.60, 160.87, 189.45; exact mass calcd. for $C_{16}H_{17}NO_2$ ($M^{\bullet+}$) 255.1259, found 255.1266 (FAB high-resolution mass spectrometry).

*Compound **11***. Elution of the column with a mixture (1:3) of ethyl acetate and petroleum ether (bp 60−80 °C) gave 740 mg (55%) of **11**. IR (neat) ν_{max} 2949, 2873, 1692, 1601, 1551, 1502, 1480, 1450, 1388, 1356, 1287, 1241, 1195, 1161, 1040, 841 cm^{-1}; ^1H NMR ($CDCl_3$) δ 2.0−2.4 (2H, m, CH_2), 2.95 (3 H, s, NCH_3), 3.4−3.8 (2H, t, NCH_2), 4.0−4.3 (2H, t, OCH_2), 6.7−7.9 (9H, m, aromatic), 10.55 (1H, s, CHO); ^{13}C NMR ($CDCl_3$) δ 26.64, 38.50, 64.92, 65.85, 112.30, 120.71, 128.53, 129.25, 135.95, 156.66, 162.96, 189.50; exact mass calcd. for $C_{17}H_{19}NO_2$ ($M^{\bullet+}$) 269.1416, found 269.1419 (FAB high-resolution mass spectrometry).

*Compound **13***. Elution with a mixture (1:4) of ethyl acetate and hexane gave 1.2 g (90%) of **13**. IR (neat) ν_{max} 2957, 2887, 2854, 1697, 1606, 1512, 1260, 1219, 1162, 1036, 834 cm^{-1}; ^1H NMR ($CDCl_3$) δ 2.0−2.4 (2H, m, CH_2), 2.95 (3H, s, NCH_3), 3.4−3.7 (2H, t, NCH_2), 4.0−4.2 (2H, t, OCH_2), 6.6−8.0 (9H, m, aromatic), 9.90 (1H, s, CHO); ^{13}C NMR ($CDCl_3$) δ 26.64, 37.89, 38.45, 64.95, 103.88, 112.21, 114.71, 116.35, 129.18, 131.96, 149.14, 163.85, 190.70; exact mass calcd. for $C_{17}H_{19}NO_2$ ($M^{\bullet+}$) 269.1416, found 269.1419 (FAB high-resolution mass spectrometry).

General Method of Synthesis of Fullerene−Aniline Dyads (2−4). A mixture of C_{60} (0.2 mmol), *N*-methyl,*N*-{(formylphenoxy)alkyl}-aniline (0.2 mmol) and *N*-methylglycine (0.2 mmol) in toluene (145 mL) was stirred under reflux for 10 h. The reaction mixture was cooled, and removal of the solvent under reduced pressure gave a solid residue, which was chromatographed over silica gel (100−200 mesh) to give the appropriate dyads.

*Dyad **2***. Elution with a mixture (1:3) of toluene and petroleum ether (bp 60−80 °C) gave 58 mg (40%) of unchanged C_{60} followed by 58 mg (48%) of **2**, mp > 400 °C; IR (KBr) ν_{max} 2940, 2869, 2785, 1606, 1568, 1509, 1473, 1429, 1363, 1336, 1301, 1245, 1176, 1035, 746 cm^{-1}; ^1H NMR ($CDCl_3$) δ 2.05 (2H, t, CH_2), 2.80 (3H, s, NCH_3), 2.92 (3H, s, NCH_3), 3.54 (2H, t, anilinic NCH_2), 4.01(2H, t, OCH_2), 4.25 (1H, d, CH of pyrrolidine), 4.88 (1H, s, CH of pyrrolidine), 4.98 (1H, d, CH of pyrrolidine), [6.58−6.75 (m), 6.96 (d), 7.13−7.29 (m) and 7.63−7.79 (s)] (9H, aromatic); ^{13}C NMR ($CDCl_3$) δ 26.85, 29.74, 38.43, 40.00, 49.37, 65.31, 70.01, 79.14, 83.19, 112.17, 114.55, 116.19, 129.19, 130.49, 135.79, 140.15, 142.12, 142.56, 145.24, 145.48, 145.94, 146.14, 153.66, 154.11, 158.92; exact mass calcd. for $C_{79}H_{24}N_2O$ ($M^{\bullet+}$) 1017.1967, found 1017.1989 (FAB high-resolution mass spectrometry).

SCHEME 1

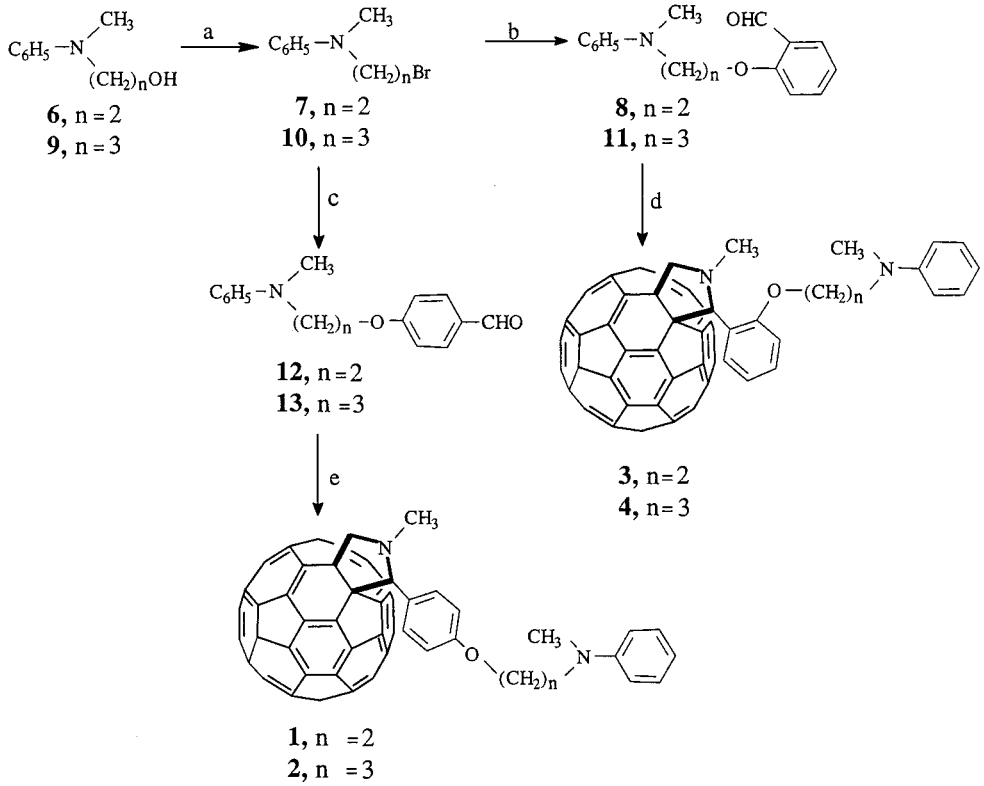

(a) PBr_3/CH_2Cl_2 (b) K_2CO_3/ *o*-OH C_6H_4 CHO/acetone, reflux

(c) K_2CO_3/ *p*-OH C_6H_4 CHO/acetone, reflux

(d), (e) C_{60}, N-methylglycine, heat

*Dyad **3***. Elution of the column with a mixture (1:3) of toluene and hexane gave 65 mg (45%) of unchanged C_{60} followed by 50 mg (45%) of the dyad **3**; mp > 400 °C; IR (KBr) ν_{max} 2932, 2866, 2786, 1602, 1500, 1455, 1361, 1338, 1247, 1184, 1107, 1036, 749 cm^{-1}; ^1H NMR ($CDCl_3$) δ 2.77 (3H, s, NCH_3), 3.02 (3H, s, NCH_3), 3.53−3.61 (1H, m, anilinic NCH), 3.64−3.71 (1H, m, anilinic NCH), 3.79−3.85 (1H, m, OCH), 4.21−4.29 (2H, m, OCH and CH of pyrrolidine), 4.95 (1H, d, CH of pyrrolidine ring), 5.52 (1H, s, CH of pyrrolidine ring), [6.70−6.81 (m), 6.68 (d), 7.10 (t), 7.14−7.32 (m) and 7.98 (d)] (9H, aromatic); ^{13}C NMR ($CDCl_3$) δ 38.57, 39.84, 51.70, 64.86, 69.01, 69.60, 75.11, 86.54, 111.30, 112.46, 116.91, 121.47, 129.01, 129.26, 129.82, 135.95, 136.43, 139.15, 140.02, 141.70, 141.94, 142.09, 142.43, 142.92, 144.24, 144.44, 144.80, 145.12, 145.26, 145.50, 145.68, 145.99, 147.09, 148.69, 153.62, 156.97; exact mass calcd. for $C_{78}H_{22}N_2O(M^{\bullet+})$ 1002.1732, found 1002.1713 (FAB high-resolution mass spectrometry).

*Dyad **4***. Elution of the column with a mixture (1:3) of toluene and hexane gave 60 mg (45%) of unchanged C_{60} followed by 57 mg (48%) of the dyad **4**; mp > 400 °C; IR (KBr) ν_{max} 2939, 2862, 2787, 1607, 1548, 1500, 1453, 1285, 1245, 1190, 1104, 1045, 754 cm^{-1}; ^1H NMR ($CDCl_3$) δ 1.89−1.91 (2H, m, CH_2), 2.82 (3H, s, NCH_3), 2.96 (3H, s, NCH_3), 3.51 (2H, t, anilinic NCH_2), 3.72−3.88 (1H, m, OCH), 3.98−4.11 (1H, m, OCH), 4.31 (1H, d, CH of pyrrolidine), 5.00 (1H, d, CH of pyrrolidine), 5.57 (1H, s, CH of pyrrolidine), [6.65−6.81 (m), 6.90 (d),7.07−7.32 (m), 7.99 (d)] (9H, aromatic); ^{13}C NMR ($CDCl_3$) δ 26.78, 29.71, 38.62, 40.18, 49.85, 65.78, 69.98, 75.85, 91.32, 111.48, 112.43, 116.41, 121.24, 128.14, 129.06, 134.82, 135.88, 135.92, 135.94, 138.25, 138.27, 138.30, 138.91, 141.29, 141.35, 141.63, 141.88, 142.64, 142.69, 142.74, 144.20, 144.50, 144.62, 145.29, 146.07, 146.82, 147.47, 149.16, 153.82, 153.88, 155.21, 156.81, 157.37; exact mass calcd. for $C_{79}H_{24}N_2O(M^{\bullet+})$ 1017.1967, found 1017.1987 (FAB high-resolution mass spectrometry).

Laser Flash Photolysis. Nanosecond laser flash photolysis experiments were performed with a Laser Photonics PRA/model UV-24 nitrogen laser system (337 nm, 2 ns pulse width, 2−4 mJ/pulse) with front face excitation geometry. A typical experiment consisted of a series of 2−3 replicate shots per single measurement. The average signal was processed with an LSI-11 microprocessor interfaced with a VAX computer. Details of the experimental set up can be found elsewhere.[13] Lifetime measurements were carried out using a PTI Laser Stobe Fluorescence lifetime system and a nitrogen laser system (PTI model GL-3300) was used as excitation source. The emission decay was monitored at 715 nm.

Results and Discussion

Computational Studies. The geometry of the different conformers was evaluated using the Sybyl force field method.[14] Computational studies suggest that the most stable conformations in the case of para-substituted dyads (**1** and **2**) are the extended ones, while both the ortho-substituted dyads (**3** and **4**) possess a folded conformation. Representative examples of structures (**2** and **4**) are displayed in Figure 1. Based on these calculations, the edge to edge distance between the anilinic nitrogen and C_{60} is found to be much larger for the para-substituted compounds (9.48 Å for **1** and 10.01 Å for **2**) as compared to the ortho-substituted compounds (3.28 Å for **3** and 4.01 Å for **4**). Over the entire spherical structure of C_{60}, the π-electron cloud is more or less available and this particular feature

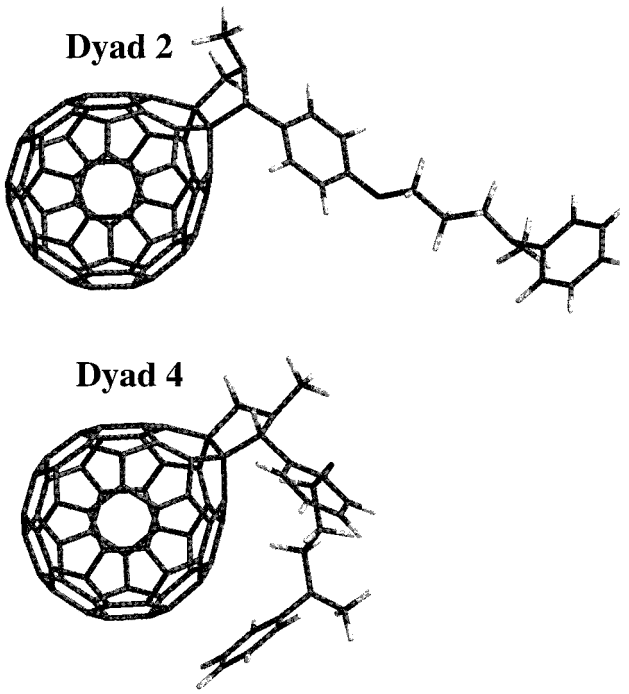

Figure 1. Minimized structure of para- and ortho-substituted dyads: (a) **2**, (b) **4**.

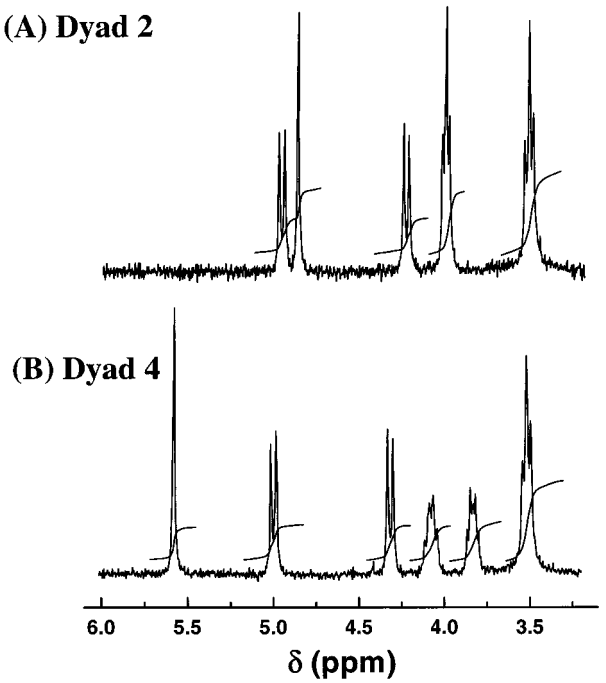

Figure 2. ^{1}H NMR (300 MHz) spectra (δ 3.2−6.0 ppm) of para-substituted dyad **2** (A) and ortho-substituted dyad **4** (B).

enhances the probability of accepting an electron through space in the folded conformation.

^{1}H NMR Studies. Further information regarding the folding of the anilinic group to the proximity of C_{60} was obtained by comparing the ^{1}H NMR spectrum (300 MHz) of the para- and the ortho-substituted dyads. Figure 2 illustrates the ^{1}H NMR spectra, in the region 3.2−6.0 ppm, for the para-substituted dyad **2** and the ortho-substituted dyad **4**. The triplets observed at 3.54 and 4.01 ppm for the para-substituted dyad **2** (Figure 2, spectrum A) are assigned to the NCH_2 (anilinic) and OCH_2 protons, respectively. Interestingly, the OCH_2 protons are observed as two separate multiplets in the case of the ortho-substituted dyads **3** and **4** (Figure 2, spectrum B). For the ortho-substituted dyad **4**, having three methylene groups, the NCH_2 protons are observed as a triplet whereas for the ortho-substituted dyad **3**, having two methylene groups, the NCH_2 protons are observed as two separate multiplets. Such effects are not observed in the case of ortho-substituted derivatives of the *N*-methyl,*N*-{(formylphenoxy)alkyl}anilines, **8**[8a] and **11** (for details, see Experimental Section). The difference in the splitting pattern, observed for the ortho-substituted dyads may be, originating from the spatial interactions of the π-electrons of C_{60} (as well as phenyl group) and the methylene groups, indicative of the proximity of C_{60} and anilinic donor group.

The doublets at 4.25 and 4.98 ppm correspond to the exo and endo protons of the pyrrolidine ring of the para-substituted dyad **2**, and their positions remain more or less the same for the ortho-substituted dyad **4** (Figure 2, spectrum A and B). The singlet observed at 4.88 ppm for the para-substituted dyad **2** is due to the methyne proton of the pyrrolidine ring and a large downfield shift is observed for this proton, in the case of the ortho-substituted dyad **4**. (Note that the aldehyde protons of the ortho-substituted derivatives of the *N*-methyl,*N*-{(formylphenoxy)-alkyl}anilines (**8**[8a] and **11)** are more deshielded than the para-substituted derivative (**12** and **13),** and details are given in the Experimental Section.) These effects could be due to the anisotropic effect of the oxygen of the *ortho*-phenoxy group.

Absorption and Emission Characteristics of Dyads. Functionalized fullerenes such as methanofullerenes and pyrrolidinofullerenes possess a weak absorption band around 700 nm, and the exact nature of this band is still being debated. An early study has suggested that the 700 nm band in the case of methanofullerenes originates from one of the orbitally forbidden transition of C_{60} or from the spin-forbidden transition to the lowest triplet state.[15a] Guldi and Maggini have assigned the 700 nm band of *N*-methylpyrrolidinofullerene (model compound **5)** to the $0 \rightarrow {}^*0$ absorption band.[15b] Another report suggests that the lone pair of electrons on nitrogen is less available in the case of fulleropyrrolidines.[15c] Through-space interactions of the nitrogen lone pair with the fullerene π systems was experimentally confirmed through acid−base studies and from the reaction rates of the alkylation of the pyrrolidine nitrogen by methyl iodide.[15c]

All of the dyads in the present investigation possess a similar long wavelength band at ∼700 nm, which are partially influenced by the addition of trifluoroacetic acid (TFA) (see ref 15d, for details). This observation suggests that protonation of the anilinic nitrogen is responsible for the partial disappearance of the absorption band. Similar observations have also been reported earlier by Williams et al.,[4a] for rigid donor−bridge−C_{60} dyads. Studies have shown that fullerenes and functionalized fullerenes have a strong tendency to form ground state intermolecular charge transfer complexes with aliphatic and aromatic amines.[16] Nakamura et al. have investigated the intermolecular CT complex formation between a C_{60}−*o*-quinodimethane and *N*,*N*-dimethylaniline (DMA).[16e] It is concluded that the DMA molecule can move freely in solvent and overlap the C_{60} surface, leading to the CT complex. We have carried out the concentration dependency, to check the Beer−Lambert law, in the case of dyad **1**. The absorption band at 700 nm increased linearly with the concentration of the dyad, thus ruling out the possibility of the formation of any intermolecular charge transfer. Moreover, the 700 nm absorption band can be seen even in dilute solutions (< 5 μM). Based on these observations, we can attribute part of the 700 nm band of dyads **1**−**4** to a weak intramolecular charge transfer absorption that results from the

TABLE 1: Fluorescence Quantum Yield (ϕ_f) of the Dyads 1−4 in Various Solvents

	Φ_f (10^4)			
solvent	1	2	3	4
toluene	6.9	6.8	6.7	6.6
dichloromethane	4.4	3.3	1.7	1.0
benzonitrile	3.1	3.1	0.2	0.25

ground state interaction between the lone pair of anilinic nitrogen and fullerene π-electron systems.

The fluorescence properties of the dyads were investigated using solvents of widely varying polarity (Table 1). The fluorescence spectrum and the quantum yield of the dyads **1**−**4** in nonpolar solvents (e.g., toluene) remained the same as that of the model compound **5**[17] (Figure 3A). These results indicated that the singlet excited state properties of the dyads are unaffected in nonpolar solvents.

A decrease in fluorescence quantum yield was observed with increasing solvent polarity for all the dyads under investigation (Table 1). The decrease in fluorescence quantum yield indicates that a charge transfer route (Reaction 3) competes quite efficiently with other deactivation routes for the deactivation of the singlet excited state (Reactions 1 and 2).[18] These observations are in line with the dependence of photoinduced electron transfer on the polarity of the medium for other fullerene based donor−acceptor dyad molecules.[4−7]

$$^1(C_{60}\text{−aniline})^* \rightarrow (C_{60}\text{−aniline}) + h\nu \quad (1)$$

$$^1(C_{60}\text{−aniline})^* \rightarrow {}^3(C_{60}\text{−aniline})^* \rightarrow (C_{60}\text{−aniline}) \quad (2)$$

$$^1(C_{60}\text{−aniline})^* \rightarrow (C_{60}{}^{\bullet-}\text{−aniline}^{\bullet+}) \quad (3)$$

One of the interesting observations in the present study is the marked decrease in the fluorescence yield, observed in the case of ortho-substituted compounds in polar solvents (Table 1 and Figure 3B). This effect is attributed to the folding of the aniline group in ortho-substituted dyads, which in turn results in an increase in the probability of electron transfer. To confirm this effect, we have further compared the fluorescence lifetimes of ortho- and para-substituted dyads.

Fluorescence Lifetime Measurements. Fluorescence lifetimes of the dyads **1**−**4** were measured in toluene and benzonitrile, respectively. Representative fluorescence decay profiles of the para-substituted dyad **1** and ortho-substituted dyad **3**, in toluene and benzonitrile solutions, are presented in Figure 4. The fluorescence decay profiles of the dyads **1**−**4** and the model compound **5** were analyzed by the deconvolution method using a single-exponential decay function (see the fitted curves in Figures 4A and B). The singlet lifetimes of the dyads **1**−**4** and model compound **5** were found to be nearly identical (τ_s = 1.3 ± 0.1 ns) in toluene. In benzonitrile solutions the para-substituted dyads, **1** and **2**, exhibited fluorescence lifetimes of 0.90 and 0.70 ns, respectively, whereas the ortho dyads **3** and **4** possess much shorter lifetimes (<0.30 ns). The decrease in the singlet lifetimes observed for the ortho-substituted dyads is in tune with decrease in the fluorescence quantum yeilds (compare Figures 3B and 4B and the ϕ_f and τ_s values in Tables 1 and 2, respectively). The rate constants and quantum yields for charge separation (k_{cs} and ϕ_{cs})[19] in excited singlet dyad molecules were estimated from the corresponding fluorescence lifetimes of the dyads and the model compound. These results are summarized in Table 2.

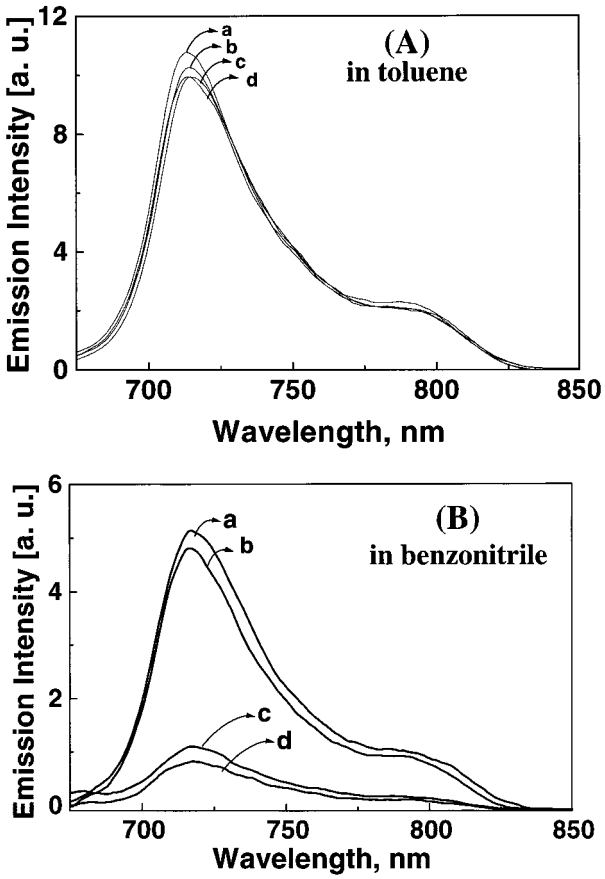

Figure 3. (A) Emission spectra of fullerene-aniline dyads **1**−**4** in toluene: (a) **1**, (b) **2**, (c) **4**, and (d) **3**. (B) Emission spectra of fullerene−aniline dyads **1**−**4** in benzonitrile: (a) **1**, (b) **2**, (c) **4**, and (d) **3** (absorbance of the solutions was adjusted to 0.1 at the excitation wavelength, 470 nm).

The short fluorescence lifetimes, observed in polar solvents, are again indicative of reductive quenching of the singlet excited state. However, the difference in the rate constants and quantum yields of charge separation (Table 2) between the ortho- and para-substituted dyads highlight the effect of orientation of the aniline donor moiety as an important factor in controlling the rate of forward electron transfer. The large ϕ_{cs} values observed for the ortho-substituted compounds (>75%) arise from the decrease in the donor−acceptor distance caused by the folding of the aniline group. As shown earlier,[20] a specific orientation between the donor and acceptor moieties in the dyad molecules is necessary for achieving an efficient electron transfer in the excited state. In the case of fullerene−aniline dyads **3** and **4**, the folding of the anilinic group, in close proximity to the π cloud of C_{60}, is sufficient to achieve an efficient charge transfer.

Intersystem Crossing vs Photoinduced Charge Separation. We have performed nanosecond laser flash photolysis experiments (using 337 nm laser pulse as the excitation source) in two solvents of differing polarity, viz., toluene (ϵ = 2.38) and benzonitrile (ϵ = 25.2), to investigate the different photochemical processes (viz., reactions 2 and 3) and characterize the intermediates formed.

Transient absorption spectra (350−1100 nm region) of the dyads (**1**−**4**) in toluene were recorded following 337 nm laser pulse excitation. The difference absorption spectra showed two absorption bands at 370 and 700 nm, and their spectral features are similar to those obtained with the model compound **5**. A representative example of time-resolved transient spectra recorded following 337 nm laser pulse excitation of **2** in deaerated

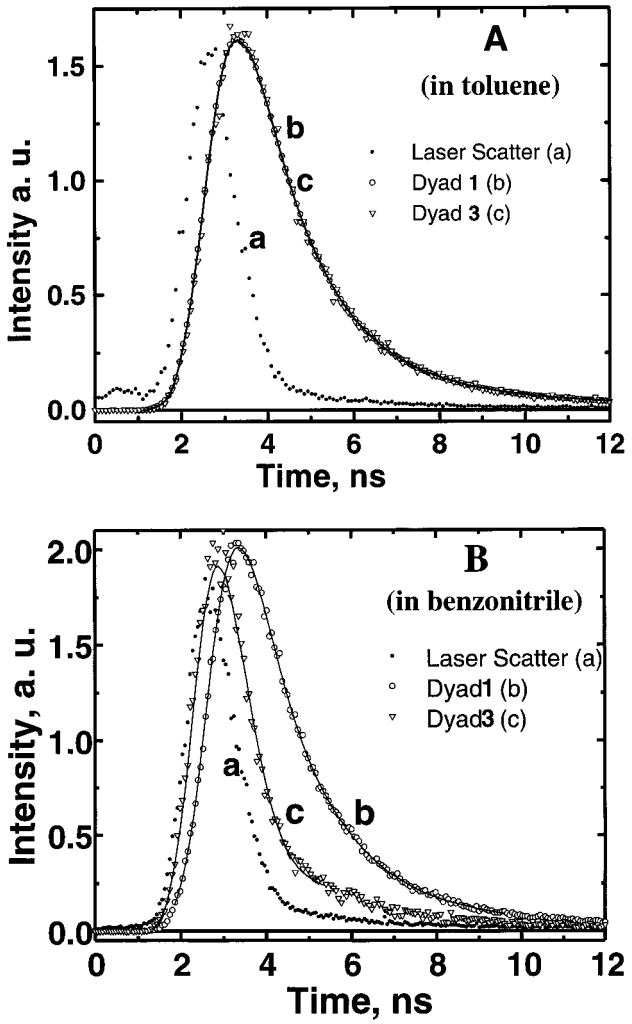

Figure 4. Fluorescence decay profiles for the para-substituted fullerene−aniline dyad (**1**) and ortho-substituted fullerene−aniline dyad (**3**) in (A) toluene and (B) benzonitrile.

TABLE 2: Single and Triplet Excited State Properties[a,b] of the Fullerene−Aniline Dyads 1−4

	toluene			benzonitrile				
dyad	τ_s(ns)[c]	τ_T(μs)	ϕ_T	τ_s(ns)[c]	τ_T(μs)	k_{cs} (10^9s^{-1})	ϕ_{cs}	ϕ_T
1	1.27	16.2	0.92	0.90	8.5	0.35	0.32	0.67
2	1.20	13.2	0.95	0.70	7.4	0.67	0.47	0.49
3	1.25	13.4	0.95	<0.30	2.2	>2.5	>0.77	0.18
4	1.14	14.4	0.95	<0.30	6.6	>2.5	>0.77	0.15

[a] τ_s anb τ_T are the lifetimes of the singlet and triplet excited states; ϕ_T and ϕ_{cs} are the quantum yield of the triplet excited state and the charge separation; k_{cs} is the rate constant for the charge separation (ref 19). [b] Photophysical properties of model compound were reported earlier (ref 21). [c] Fluorescence decay profile of the dyads **1**−**4** and model compound **5** were analyzed by the deconvolution method using a single-exponential decay function (see the fitted curves in Figure 4A and B). The χ^2 values for the fitting was within the error limits ($\chi^2 = 1.0 \pm 0.1$).

toluene are shown in Figure 5. Based on previous reports,[8] we can assign these absorption bands to the triplet excited state of the dyads. Absorption−time profiles of optically matched solutions (absorbance at 337 nm = 0.7) of the para-substituted dyad **2** and the ortho-substituted dyad **4**, in toluene and benzonitrile, are compared in Figure 6. Lifetimes of the triplet excited states of the dyads in toluene were estimated by fitting the absorption−time decay curves to first-order kinetics, which yielded values in the range of 13 to16 μs.

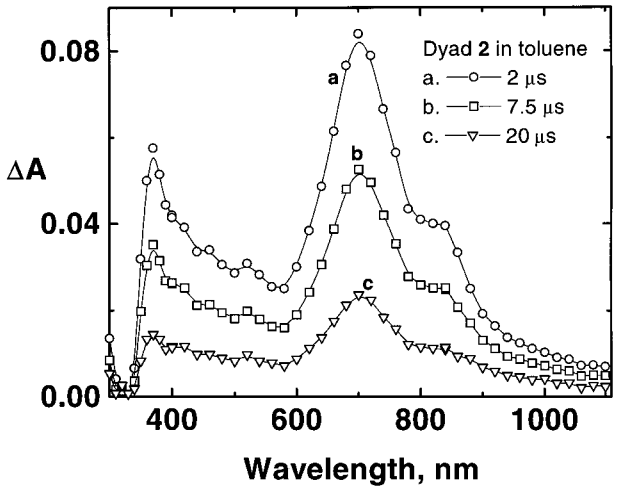

Figure 5. Difference absorption spectra, recorded after 337 nm laser pulse excitation of the dyad **2** (~30 μM) in deoxygenated toluene in the visible−NIR region.

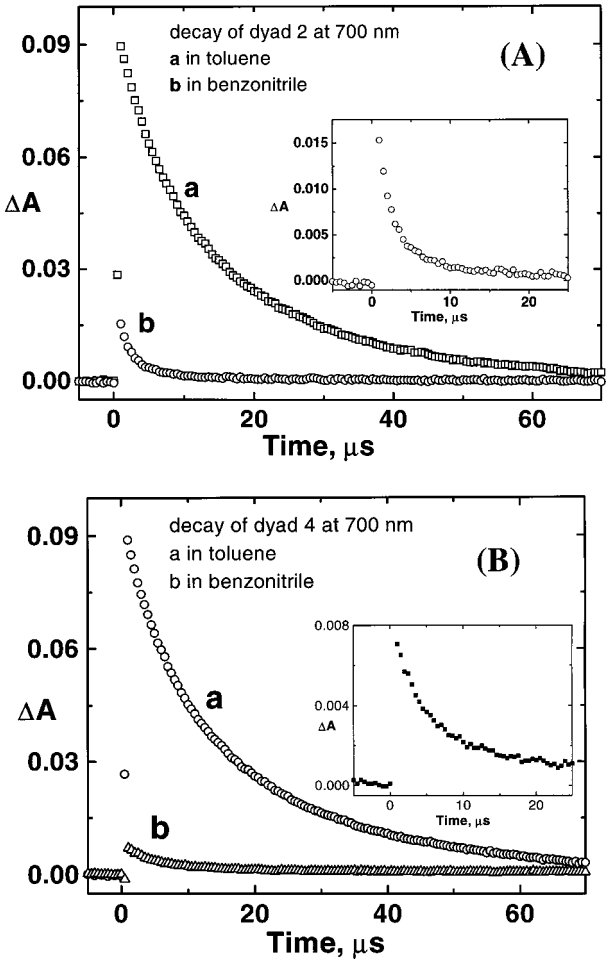

Figure 6. The absorption−time decay profile at 700 nm following 337 nm laser pulse excitation of the fullerene−aniline dyad (~30 μM) in deoxygenated benzonitrile: (A) dyad **2** and (B) dyad **4**. Insets show the transient absorption spectrum of the dyads in benzonitrile.

Quantum yields of the triplet excited states were estimated by a relative method using model compound **5** as actinometer ($\phi_T = 0.95$).[21] In toluene solutions, all of the dyads (**1**−**4**) exhibited efficient intersystem crossing to yield a triplet quantum yield of nearly unity (Table 2). These results indicate that the intersystem crossing is the dominant pathway for the deactivation of the excited singlet state in a nonpolar solvent such as

toluene. It may be noted that this conclusion was similar to the one drawn from the fluorescence measurements. In the case of polar solvents such as benzonitrile, a drastic decrease in the triplet quantum yield was evident for all of the dyads (Table 2). The decrease in the fluorescence yields and lifetimes as well as the lower triplet yields observed in benzonitrile, relative to toluene, are supportive of an intramolecular electron transfer from the singlet excited dyads. The results of the triplet excited state properties of the dyad molecules in toluene and benzonitrile are summarized in Table 2.

It is noteworthy that the sums of triplet quantum yield and charge transfer efficiency from the singlet excited state for the four dyads is around unity in each case. (Please note that Φ_T and Φ_{CT} were independently determined using transient absorption and fluorescence lifetime measurements, respectively.) Therefore, intersystem crossing and photoinduced electron transfer are the only two major pathways with which the excited singlet state deactivates (reactions 2 and 3). In toluene solutions, the high triplet quantum yield ($\Phi_T = 0.95$) observed for dyads **1**−**4** reflects the dominance of intersystem crossing over the electron transfer pathway (reaction 2). Both steady state emission and fluorescence lifetime measurements indicate that the forward electron transfer is quite efficient in benzonitrile for all of the dyads employed in the present investigation. This feature becomes especially prominent for ortho-substituted dyads **2** and **4**, and the forward electron transfer process becomes the major pathway ($\Phi_{CT} = 0.77$). The enhanced rate of forward electron transfer and the high quantum yield of charge separation (Table 2) observed in the case of the ortho-substituted dyads can be attributed to the folding of the aniline group. The computational calculations and ^{1}H NMR studies, discussed in an earlier section, support this argument. Such a conformation decreases the donor−acceptor distances in the ortho-substituted dyads, thus favoring the electron transfer.

Electron Transfer Products. The fate of electron transfer products via reaction 3, (radical anion of C_{60} and the radical cation of aniline) in dyads **1**−**4**, was further probed by monitoring the absorbance in the near-infrared (NIR) region using nanosecond flash photolysis. Earlier studies have shown that the radical cation of aniline exhibits a characteristic absorption around 460 nm.[4a] However, in the present case, it is not possible to obtain clear evidence for the formation of the radical cation, due to the dominance of the triplet absorption in this spectral region (Figure 5 and Table 2). The radical anion of C_{60}, the other charge-separated species formed, can be readily detected from its characteristic NIR (∼1000 nm) band. Earlier studies using pulse radiolysis have indicated that the radical anion of the dyad **1** exhibits a prominent absorption band at 400 and 1005 nm.[8a]

Time-resolved transient absorption spectra recorded following 337 nm laser pulse excitation of dyads **2** and **4** are shown in Figure 7. The appearance of an absorption band at 1010 nm in both these experiments confirmed the formation of the C_{60} radical anion. However, the absorption arising from the C_{60} radical anion was not so prominent in dyads **1** and **3** (in benzonitrile) and could not be detected using nanosecond laser flash photolysis. Although the rates and quantum yields of charge separation (k_{cs} and Φ_{cs}) for both the ortho-substituted dyads (**3** and **4)** are similar (Table 2), the extent of charge stabilization in these two cases is different. The values of k_{cs} and Φ_{cs}, as determined from fluorescence measurements, reflect only the forward electron transfer. On the other hand, the stabilized electron transfer products observed in nanosecond laser flash photolysis also reflect charge recombination. The

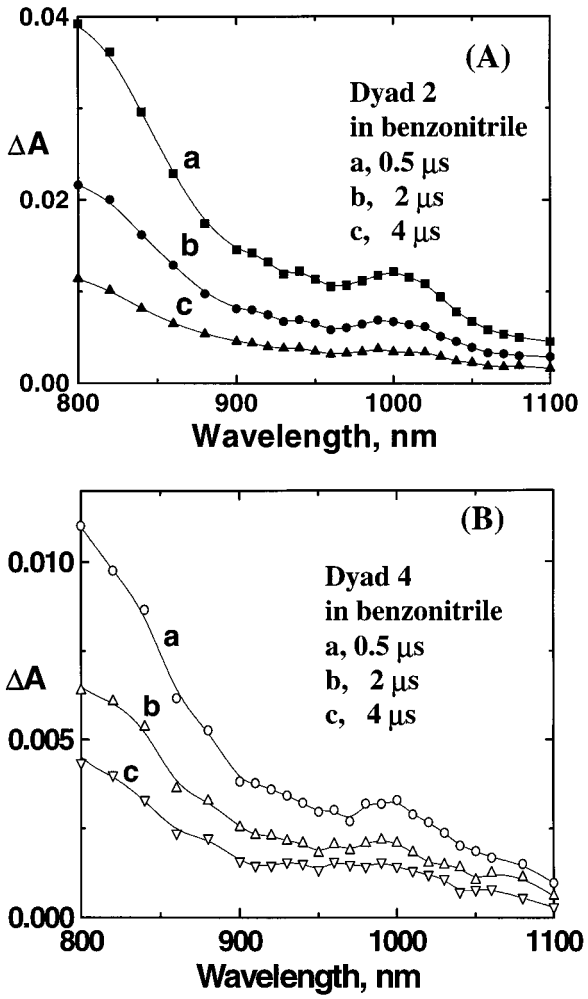

Figure 7. Difference absorption spectra, recorded after 337 nm laser pulse excitation of the fullerene−aniline dyads (∼30 μM) in deoxygenated benzonitrile: (A) dyad **2** and (B) dyad **4**.

failure to observe the C_{60} radical anion following the excitation of **1** and **3** essentially indicates the dominance of faster charge recombination in these dyads.

In the dyad systems **2** and **4**, the anilinic donor is linked to the para as well as ortho positions of phenyl group of 1-methyl-2-phenylpyrrolidinofullerene through three methylene chains. In the dyad systems **1** and **3**, the donor and acceptor groups are linked together by two methylene groups. Based on the flash photolysis experiments we can conclude that the charge recombination process in these dyads is dependent on the length of the alkyl chain. The stability of the radical pairs, in the case of dyads **2** and **4**, is likely to arise from the presence of an additional methylene group linking the donor and acceptor. Such an increase in the number of carbon atoms in the alkyl chain is likely to provide an additional degree of freedom for conformational rearrangements of fullerene and aniline moieties.

The charge-separated intermediates formed can recombine to yield either the excited triplet state of the dyad or the ground state (reactions 4 and 5)

$$(C_{60}^{\bullet-}-\text{aniline}^{\bullet+}) \rightarrow {}^3(C_{60}-\text{aniline})^* \quad (4)$$

$$(C_{60}^{\bullet-}-\text{aniline}^{\bullet+}) \rightarrow (C_{60}-\text{aniline}) \quad (5)$$

If the charge-separated state recombines to yield the triplet excited state (reaction 4), one would expect a growth in the triplet state absorption at 700 nm in parallel with the decay of

radical ions. Both picosecond[8a] and nanosecond laser flash studies did not show any growth component corresponding to the charge recombination. Hence we rule out reaction 4 as the major deactivation pathway for the recombination of charge separated pairs and conclude that the recombination mainly proceeds via reaction 5.

The solvent may also modify to some extent the reported conformations (Figure 1). Despite such reservations about the exact validity of the structures, the experimental evidence based on steady state and time-resolved fluorescence spectroscopy indicate the attachment of the anilinic group on the ortho positions of phenyl group of 1-methyl-2-phenylpyrrolidinofullerene promotes the forward electron transfer process via a through-space mechanism. We also attempted to calculate the free energy changes for dyads **1**−**4** within the frame of the dielectric continuum model. The latter model accounts for the sum of the ionic radii (radical cation and radical anion) and subtracts there from the spatial separation of the donor/acceptor couple. The close separation in dyads **3** (3.28 Å) and **4** (4.01 Å) indicates a van der Waals contact between the two moieties and therefore makes the conclusions derived from these calculations rather uncertain. We can conclude only that the free energy changes in the ortho-substituted dyads are much larger than in the para-substituted ones, since, based on the close contact, a through-space electron transfer should prevail over the through-bond electron transfer.

Despite the high efficiency of charge separation in benzonitrile solutions we were able to detect the C_{60} radical anion only in the case of dyads **2** and **4**, indicating that the charge recombination process is more depend on the length of the alkyl chain. In general, fast charge recombination[22] is a major limiting factor in achieving a long-lived charge separated pair in these donor acceptor systems. An elegant approach to suppress such a recombination will be to employ clusters of fullerene-based dyads in mixed solvents.[8b] By clustering these fullerene-donor dyads, it is possible to induce the hopping of electron to the adjacent fullerene moieties which in turn enhances charge stabilization.

Conclusions

The orientation-dependent electron transfer studies are significant in fullerene-based systems because of the spherical cage and the π-electron cloud that surrounds it. The experimental evidence based on steady state and time-resolved spectroscopy is in agreement with computational studies (folded conformation for the ortho-substituted derivatives and extended conformation for para-substituted derivatives). The marked increase in the rate constants and quantum yields of charge separation observed in the present case for ortho-substituted dyads in benzonitrile is attributed to the folding of the anilinic group. The folding of the anilinic group, in close proximity to the π cloud of C_{60}, enhances the probability of forward electron transfer for the ortho-substituted fullerene−aniline dyads via a through-space mechanism.

Acknowledgment. The authors thank the Office of Basic Energy Science of the Department of Energy, the Council of Scientific and Industrial Research, Government of India, and the Jawaharlal Nehru Center for Advanced Scientific Research, Bangalore for their support of the work described herein. This is contribution no. RRLT-PRU 95 from RRL, Trivandrum and NDRL 4137 from Notre Dame Radiation Laboratory.

References and Notes

(1) (a) Deisenhofor, J.; Michel, H.; *Angew Chem. Int. Ed. Engl*. **1989**, *28*, 829. (b) Huber, R.; *Angew. Chem., Int. Ed. Engl*. **1989**, *28*, 848.

(2) Balzani, V.; Maggi, L.; Scandola, F. In *Supramolecular Photochemistry*, Balzani, V., Ed.; Reidel: Holland, 1987; pp 1−28.

(3) (a) Imahori, H.; Sakata, Y.; *Adv. Mater*. **1997**, *9*, 537. (b) Martin, N.; Sanchez, B.; Illescas, B.; Perez, I. *Chem. Rev*. **1998**, *98*, 2527. (c) Sun, Y.-P. In *Molecular and Supramolecular Photochemistry, Vol. 1, Organic Photochemistry*; Ramamurthy, V., Schanze, K. S., Eds.; Marcel Dekker: New York, 1997; pp 325−390. (d) Foote, C. S. In *Topics in Current Chemistry; Electron Transfer 1*; Matty, J., Ed.; Springer-Verlag: Berlin, 1994; p 347. (e) Kamat, P. V.; Asmus, K.-D. *Interface* **1996**, *5*, 22. (f) Zhou, F.; Jehoulelt, C.; Bard, A. J. *J. Am. Chem. Soc*. **1992**, *114*, 11004. (g) Dubois, D. K.; Kadish, K. M.; Flanagan, S.; Haufler, R. E.; Chibante, L. P. E. Wilsson, L. F. *J. Am. Chem. Soc*. **1992**, *114*, 3978. (h) Arbogast, J. W.; Foote, C. S.; Kao, M. *J. Am. Chem. Soc*. **1992**, *114*, 2277.

(4) (a) Williams, R. M.; Koeberg, M.; Lawson, J. M.; An, Y.-Z. Rubin, Y.; Paddon-Row, M. N.; Verhoeven, J. W. *J. Org. Chem*. **1996**, *61*, 5055. (b) Williams, R. M.; Zwier, J. M.; Verhoeven, J. W. *J. Am. Chem. Soc*. **1995**, *117*, 4093

(5) (a) Kuciauskas, D.; Linddell, P. A.; Moore, A. L.; Moore, T. A.; Gust, D. *J. Am. Chem. Soc*. **1998**, *120*, 10880. (b)Liddell, P. A.; Kuciauskas, D.; Sumida, J. P.; Nash, B.; Nguyen, D.; Moore, A. L.; Moore, T. A.; Gust, D. *J. Am. Chem. Soc*. **1997**, *119*, 1400. (c) Kuciauskas, D.; Lin, S.; Seely, G. R.; Moore, A. L.; Moore, T. A.; Gust, D.; Drovetskaya, T.; Reed, C. A.; Boyd, P. D. W. *J. Phys. Chem*. **1996**, *100*, 15926. (d) Liddell, P. A.; Sumida, J. P.; Macpherson, A. N.; Noss, L.; Seely, G. R.; Clark, K. N.; Moore, A. L.; Moore, T. A.; Gust, D. *Photochem. Photobiol*. **1994**, *60*, 537. (e) Imahori, H.; Hagiwara, K.; Asoki, M.; Akiyama, T.; Taniguchi, S. Okada, T.; Shirakawa, M.; Sakata, Y. *J. Am. Chem. Soc*. **1996**, *118*, 11771. (f) Imahori, H.; Yamada, K.; Hasegawa, M.; Taniguchi, S. Okada, T.; Sakata, Y. *Angew. Chem., Int. Ed. Engl*. **1997**, *36*, 2626.

(6) Baran, P. S.; Monaco, R. R.; Khan, A. U.; Schuster, D. I.; Wilson, S. R. *J. Am. Chem. Soc*. **1997**, *119*, 8363.

(7) (a) Guldi, D. M.; Maggini, M.; Scarrano, G.; Prato, M. *J. Am. Chem. Soc*. **1997**, *119*, 974. (b) Sariciftci, N. S.; Wudl, F.; Heeger, A. J.; Maggini, M.; Scarrano, G.; Prato, M.; Bourassa, J.; Ford, F. C. *Chem. Phys. Lett*. **1995**, *247*, 510.

(8) (a) Thomas, K. G.; Biju, V.; George, M. V.; Guldi, D. M.; Kamat, P. V. *J. Phys. Chem*. **1998**, *102*, 5341. (b) Thomas, K. G.; Biju, V.; George, M. V.; Guldi, D. M.; Kamat, P. V. *J. Phys. Chem. B* **1999**, *103*, 8864.

(9) (a) Connolly, J. S.; Bolton, J. R. In *Photoinduced Electron Transfer, Part D*; Fox, M. A., Channon, M., Eds.; Elsevier: Amsterdam, 1988; pp 303−393. (b) Wasielewski, M. R. In *Photoinduced Electron Transfer, Part A*; Fox, M. A., Channon, M., Eds.; Elsevier: Amsterdam, 1988; pp 161−206. (c) Osuka, A.; Morikawa, S.; Maruyama, K.; Hirayama, S.; Minami T. *J. Chem. Soc., Chem. Commun*. **1987**, 359. (d) Fox, M. A. In *Photoinduced Electron Transfer III, Topics in Current Chemistry-159*; Mattay, J., Ed.; Springer- Verlag: Berlin, 1991; pp 67−101. (e) Gust, D.; Moore, T. A. In *Photoinduced Electron Transfer III, Topics in Current Chemistry-159*; Mattay, J., Ed.; Springer- Verlag: Berlin, 1991; pp 103−151.

(10) (a) Luo C.; Fujitsuka, M.; Huang, C.-H.; Ito, O. *J. Phys. Chem.* A. **1998**, *102*, 8716.

(11) Confirmed on a Cosmosil Buckprep HLPC column.

(12) (a) For synthesis of **5**, see: Maggini, G.; Scarrano, G. Prato, M. *J. Am. Chem. Soc*. **1993**, *115*, 9798. (b) For the preparation of **10** through a different route see, Liang, K.; Law, K.-Y.; Whitten, D. G. *J. Phys. Chem. B* **1997**, *101*, 540.

(13) Nagarajan, V.; Fessenden, F. W. *J. Phys. Chem*. **1985**, *89*, 2330.

(14) Evaluated using the Sybyl force field method of PC SPARTAN software obtained from Wavefunction, Inc.; 18401, Von Karman, Suite 370, Irvine, CA 92612.

(15) (a) For discussions on the 700 nm band observed in the case of methanofullerene derivatives see, Bensasson, R. V.; Bienvenüe, E.; Fabre, C. Janot, J.-M.; Land, E. J.; Leach, S.; Leboulaire, V.; Rassat, A.; Roux, S.; Seta, P. *Chem. Eur. J*. **1998**, *4*, 270. (b) Guldi, D. M.; Maggini M. *Gazz. Chim. Ital*. **1997**, *127*, 779. (c) Prato, M.; Maggini, M.; *Acc. Chem. Res*. **1998**, *31*, 519. (d) Protonation of the anilinic nitrogen by adding trifluoroacetic acid (25 mM) to CH_2Cl_2 solutions of dyads **2**−**4** causes a partial disappearance of the band around 700 nm. This change is completely reversed by adding pyridine (30 mM) to the above solution. The absorption spectrum of the model compound was found to be unaffected by the addition of TFA (250 mM), ruling out the possibility of a ground state charge transfer interaction.

(16) (a) Sun, Y.-P.; Ma, B.; Lawson, G. E. *Chem. Phys. Lett*. **1995**, *233*, 57. (b) Sun, Y.-P.; Bunker, C. E.; Ma, B. *J. Am. Chem. Soc*. **1994**, *116*, 9692. (c) Seshadri, R.; Rao, C. N. R.; Pal, H.; Mukherjee, T.; Mitttal, J. P. *Chem. Phys. Lett*. **1993**, *205*, 395. (d) Wang, Y. *J. Phys. Chem*. **1992**,

96, 764. (e) Nakamura, Y.; Minowa, T.; Hayashida, Y.; Tobita, S.; Shizuka, H.; Nishimura, J. *J. Chem. Soc., Faraday Trans.* **1996**, *92*, 377.

(17) Since the emission spectral profile of the dyads and spectral region of emission of model compound **5** are nearly identical, **5** was used as reference.[4,7a]

(18) An increase in fluorescence was observed on addition of trifluoroacetic acid (25 mM) to benzonitrile solution of dyads **1**−**4** (∼80% of ϕ_f of that in toluene) and is due to the protonation of the anilinic nitrogen which inhibits the electron transfer processes.

(19) (a) k_{cs} values were estimated as $1/\tau - 1/\tau_{ref}$ where τ and τ_{ref} are the lifetimes of the corresponding dyad and of the model compound **5** [τ_{ref} = 1320 ps (present study); previous reports[4,7a] τ_{ref} = 1280 ps]; (b) ϕ_{cs} values are estimated as $k_{cs}/[(1/\tau_{ref}) + k_{cs}]$.

(20) (a) Sakata, Y.; Nakashima, S.; Goto, Y.; Misumi, S.; Asahi, T.; Hagihara, M.; Nishikawa, S.; Okada, T.; Mataga, N. *J. Am. Chem. Soc.* **1989**, *111*, 8979. (b) Wasielewski, M. R.; Niemczyk, M. P.; Johnson, D. G.; Svec, W. A.; Minsek, D. W. *Tetrahedron* **1989**, *45*, 4785. (c) Sakata, Y.; Tsue, H.; Goto, Y.; Misumi, S.; Asahi, T.; Nishikawa, S.; Okada, T.; Mataga, N. *Chem. Lett.* **1991**, 1307.

(21) Luo, C.; Fujitsuka, M.; Watanabe, A.; Ito, O.; Gan, L.; Huang, Y.; Huang, C.-H. *J. Chem. Soc., Faraday Trans.* **1998**, *94*, 527.